



Short communication

Interconnected TiO₂ nanowires consisting of nanosized crystallites for high conversion efficiency in dye-sensitized solar cells with gel electrolyte

Juangang Wang^{*}, Tiedan Chen

College of Chemistry and Material Science, Huaibei Normal University, Huaibei 235000, Anhui, China

H I G H L I G H T S

- Interconnected nanowires consist of nanocrystallites (INCNCs) film was reported.
- This INCNCs film provides a large surface area for the adsorption of dye molecules.
- The INCNCs photoelectrode displays markedly high charge-collection efficiency.
- A high light-to-electricity yield of 8.20% was achieved by applying the INCNCs.

A R T I C L E I N F O

Article history:

Received 12 January 2014

Received in revised form

23 April 2014

Accepted 7 May 2014

Available online 23 May 2014

Keywords:

One-dimensional semiconductor

architectures

Interconnected nanowire consisting of

nanosized crystallites

Charge-collection efficiency

Electron transport time

A B S T R A C T

In this paper, we present a method to prepare interconnected TiO₂ nanowires consisting of nanosized crystallites (INCNCs). A high light-to-electricity conversion yield of 8.20% was achieved by applying the structure of the thin INCNCs electrode film in DSSC with gel electrolyte, much higher than 6.84% of TiO₂ nanoparticulate film with same thickness (6.5 μm).

© 2014 Elsevier B.V. All rights reserved.

1. Introduction

Dye-sensitized solar cells (DSSC) show great promise as an inexpensive alternative to conventional p–n junction solar cells [1–8]. Investigations into the various factors influencing the solar conversion efficiency in this novel approach have recently been intensified. Highly efficient solar conversions, combined with ease of manufacturing and low production costs, make the DSSC technology an attractive approach for large-scale solar energy conversion [9–16]. The highest power conversion efficiency of DSSCs with organic solvent-based electrolyte was reported to exceed 11% [17]. However, the use of organic solvent-based electrolyte also caused some practical problems, such as leakage, evaporation of solvent. At present, many attempts have been made to substitute liquid

electrolytes [18–20]. Unfortunately, DSSCs with quasi-solid/solid-state electrolytes have low conversion efficiencies compared with the liquid versions, because of the slow charge transport and high electron recombination rates in the quasi-solid/solidstate electrolytes. Recently, the use of a film constructed of one-dimensional crystalline nanowire arrays, has been found to enhance charge collection efficiency by promoting faster charge transport [21,22]. In the present work, we describe the preparation of a INCNCs structured TiO₂ membrane as the electrode in DSSCs with gel electrolyte by a simple process for the improvement of solar conversion efficiency.

2. Experimental section

2.1. Materials and methods

All chemicals (Tianjin Chemical Reagents Co.) used in our experiments were of analytical reagent grade without further

^{*} Corresponding author. Tel./fax: +86 05613803233.

E-mail address: shanxiwangjuangang@126.com (J. Wang).

purification. Fumed silica nanoparticles (12 nm primary particle size and surface area of $380 \text{ m}^2 \text{ g}^{-1}$) were purchased from Degussa. The anatase TiO_2 nanoparticles (15 nm primary particle size) were purchased from Aladdin. The film thickness was measured by using a Kosaka Lab. SE-2300 surface profilometer. Nitrogen adsorption isotherms were achieved on a Micromeritics ASAP2010 nitrogen adsorption apparatus. The Brunauer–Emmett–Teller (BET) equation was used to calculate the surface area from the adsorption branch. The surface morphology of the films was observed on a Topcon ABT-150FS scanning electron microscope (SEM). The nanowires were investigated by transmission electron microscopy (TEM, Philips CM30, operation at 200 kV). Structure phase analyses with the X-ray diffraction (XRD) method were performed on a D8-advance X-ray diffractometer (Bruker) with $\text{Cu K}\alpha$ radiation ($\lambda = 0.15418 \text{ nm}$). The XRD measurement was carried out on powders scratched from the FTO substrate. Transport and recombination properties were measured in our work using intensity-modulated photocurrent spectroscopy (IMPS) and intensity-modulated photovoltage spectroscopy (IMVS). The amount of adsorbed dye on the samples was estimated by measuring light absorption at 550 nm of the dye molecule that was dissolved from the dye-adsorbed TiO_2 films into 0.1 M NaOH aq.

2.2. Synthesis of INCNCs

The INCNCs are synthesized on FTO coated glass (Asahi Glass, $10 \text{ }\Omega/\text{square}$, $1 \times 1 \text{ cm}^2$) initially cleaned by sonication in 2-propanol, acetone, and methanol, subsequently rinsed with deionized water, and finally dried in a nitrogen stream. The FTO coated glass substrate is placed within a sealed Teflon reactor (20 mL), containing 12 mL of methanol and 2 mL of deionized water, 1 mM of glycerine, 2 mM of tetrabutyl titanate, 1 mM of titanium tetrachloride (1 M in toluene), and 1 mL of hydrochloric acid (37 wt%). A reaction temperature of 180°C is used, with reaction time lasting for 48 h. The INCNCs were then rinsed with deionized water and annealed in air at 450°C for 30 min to remove any residual organics from the TiO_2 surface and to optimize cell performance. The substrates were repeatedly introduced to fresh solution baths in order to obtain a thick film. Thicknesses of 4.6 and $6.5 \text{ }\mu\text{m}$ were achieved when repeated 3 and 4 times, as used in the current study.

2.3. Construction of nanoparticulate film

The TiO_2 nanoparticulate films were prepared by directly deposited onto FTO conductive glass substrates using doctor-blading 30 wt% powder in ethanol solution.

2.4. Synthesis of gel electrolyte

The gel electrolyte was prepared as follows. 0.5 mL of 1-Butyl-3-methylimidazolium tetrafluoroborate was mixed with 3.0 g of succinonitrile to give a clear liquid. Then a liquid electrolyte consisting of 0.5 M tetrabutylammoniumiodide (Bu_4NI) and 0.1 M I_2 in the liquid 1-Butyl-3-methylimidazolium tetrafluoroborate system was prepared. Finally, a stable gel electrolyte was obtained by mixing fumed silica nanoparticles (2 wt%) with the above liquid electrolyte through stirring and subsequently sonicating.

2.5. Fabrication of DSSCs

The INCNCs film and nanoparticulate film were immersed into a 0.3 mM solution of dye Z907 CH_3CN and t-butanol (volume ratio of 1:1) at room temperature for 12 h. 113 mg gel electrolyte was spin-coated (speed of 700 r min^{-1}) onto the dye-adsorbed TiO_2

electrode, and kept in the vacuum oven for 2 h. The counter electrode was transparent conducting optical glass on which a 200 nm thick layer of Pt was deposited by sputtering. Subsequently, the cells were sealed with thermal adhesive films for the measurement.

2.6. Photoelectrochemical measurements

Photocurrent density–voltage curves of the DSSCs were measured under standard AM 1.5 solar illumination with an intensity of $100 \pm 3 \text{ mW cm}^{-2}$ using a computerized Keithley Model 2400 SourceMeter unit. A 1000 W xenon lamp (Thermo Oriel, USA) served as the light source. The active electrode area was typically 0.10 cm^2 . Monochromatic light in the range of 400–800 nm was obtained by using a series of filters, and the incident photo to current conversion efficiency (IPCE) measurement was performed on a Keithley Model 2400 SourceMeter.

3. Results and discussion

The calculated result showed that INCNCs electrode film had high BET surface areas of $132 \text{ m}^2 \text{ g}^{-1}$, which is comparable to the BET surface area ($127 \text{ m}^2 \text{ g}^{-1}$) of the nanoparticulate electrode film used in our experiment. Fig. 1 shows scanning electron microscope top-surface images of the obtained TiO_2 film on FTO glass substrate at low and high magnification. Fig. 1a indicates that the film is well stacked with submicrometer-sized TiO_2 wires. For a clearer view, Fig. 1b presents a magnified SEM image of the INCNCs, in which the highly organized structure of the film assembled by interconnected nanowires consisting of TiO_2 nanosized crystallites. Fig. 1c displays TEM image of the interconnected nanowires. The XRD pattern of interconnected TiO_2 nanowires is shown in Fig. 1d, indicating formation of the anatase phase. Applying the Scherrer equation [23] to the anatase (101) peak at $2\theta = 25.3^\circ$ revealed an average crystallite size of 13 nm.

In dye-sensitized solar cells, the photogenerated electron transfer from photo-excited dye molecules to nanostructured semiconductor substrates needs to be sufficiently fast to compete effectively against loss processes and thus achieve high solar energy conversion. Fig. 2 compares the transport and recombination time constants for INCNCs and nanoparticulate electrode films as a function of the incident photon flux I_0 . The thicknesses of the INCNCs and nanoparticulate electrode films in the cells were about the same, at 4.6 and $4.5 \text{ }\mu\text{m}$, respectively. The cell containing the INCNCs TiO_2 electrode film exhibited a collection time constant τ_c of $7.52 \times 10^{-4} \text{ s}$ at the highest light intensity ($8.16 \times 10^{16} \text{ cm}^{-2} \text{ s}^{-1}$) and $8.20 \times 10^{-3} \text{ s}$ at the lowest light intensity ($1.42 \times 10^{15} \text{ cm}^{-2} \text{ s}^{-1}$). In contrast, the nanoparticulate electrode film exhibited τ_c of $9.36 \times 10^{-4} \text{ s}$ at $8.16 \times 10^{16} \text{ cm}^{-2} \text{ s}^{-1}$ and $1.36 \times 10^{-2} \text{ s}$ at $1.42 \times 10^{15} \text{ cm}^{-2} \text{ s}^{-1}$. The electron transport of the nanoparticulate electrode film was therefore slower than that of the INCNCs film, presumably owing to it being limited by the residence time of electrons in traps within both the particle network and the interparticle contact area. The INCNCs are good electrical conductors along the direction of the wire axes. This rapid transport provided by a INCNCs electrode film will be particularly favorable for cell designs that use quasi-solidify the liquid electrolyte, such as polymer matrixes or p-type semiconductors, in which recombination rates are high compared with those of liquid electrolyte cells.

Fig. 2b shows that the recombination time constant τ_r for the INCNCs film was several orders of magnitude larger than that of the nanoparticulate electrode film over the light-intensity range investigated. The cell containing the INCNCs TiO_2 electrode film exhibited a recombination time constant τ_r of $6.40 \times 10^{-2} \text{ s}$ at the highest light intensity ($8.16 \times 10^{16} \text{ cm}^{-2} \text{ s}^{-1}$) and 0.54 s at the lowest light intensity ($1.42 \times 10^{15} \text{ cm}^{-2} \text{ s}^{-1}$). In contrast, the

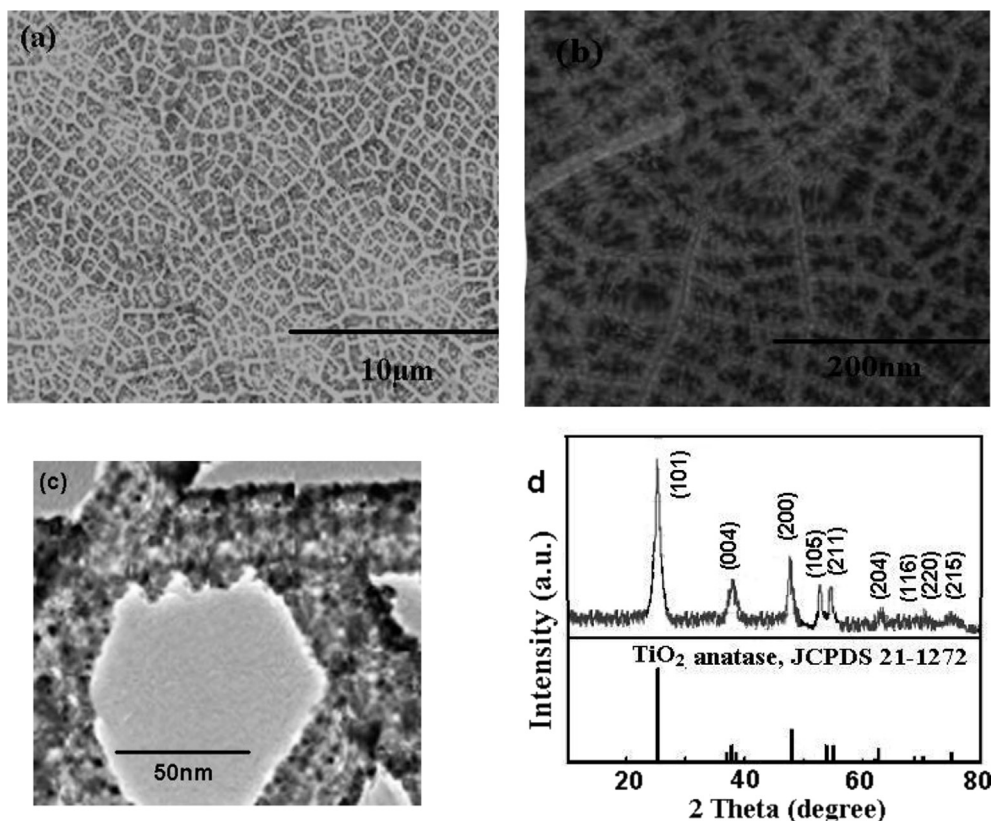


Fig. 1. Morphology of the INCNCs film. (a) SEM image of the top view of the INCNCs film. (b) A magnified SEM image of the INCNCs. (c) TEM image of INCNCs. (d) XRD pattern of the INCNCs film.

nanoparticulate electrode exhibited τ_r of 7.4×10^{-3} s at $8.16 \times 10^{16} \text{ cm}^{-2} \text{ s}^{-1}$ and 0.084 s at $1.42 \times 10^{15} \text{ cm}^{-2} \text{ s}^{-1}$. Intrinsic INCNCs surface states play an important role in this process, not only as electron traps but also as intermediate states for electron transfer to the gel electrolyte. The slower recombination could indicate that fewer potential surface recombination sites exist in INCNCs than in nanoparticulate electrode film. This therefore implies that INCNCs film can be made much thicker than nanoparticulate film for a given recombination loss, which would allow for a higher light-harvesting efficiency, especially at the long-wavelength end of the visible light and in the near-infrared region.

Fig. 3a shows the incident monochromatic photon to electron conversion efficiency (IPCE) as a function of wavelength for the TiO₂

nanowire and nanoparticulate electrode. The IPCE value reaches a maximum of approximately 81.6% for Z907 molecules on the INCNCs TiO₂ electrode, indicating that the INCNCs have broad and high light absorption and low charge recombination. The key point to the high IPCE value of the INCNCs electrode film is that the INCNCs provides a large surface area as large as that of a nanoparticulate electrode film for the adsorption of Z907 molecules, leading to high light-harvesting efficiency. While the maximum IPCE in the visible region contributed by the dye absorption are located at approximately 548 nm with a value of 68.3% for nanoparticulate electrode film. It is clear that once the dissimilarity in the transport and recombination process arising from the different structures of the INCNCs and the nanoparticulate photoelectrode

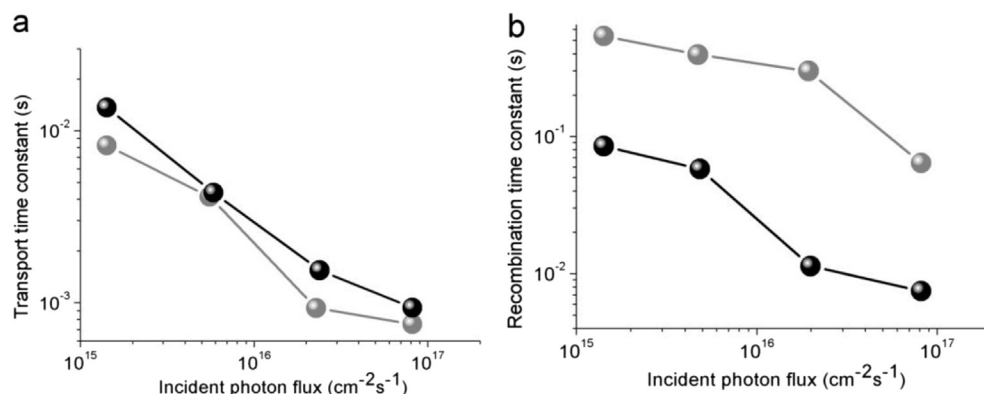


Fig. 2. Comparison of transport and recombination time constants for INCNCs and nanoparticulate DSSCs. INCNCs film = gray, nanoparticulate film = black.

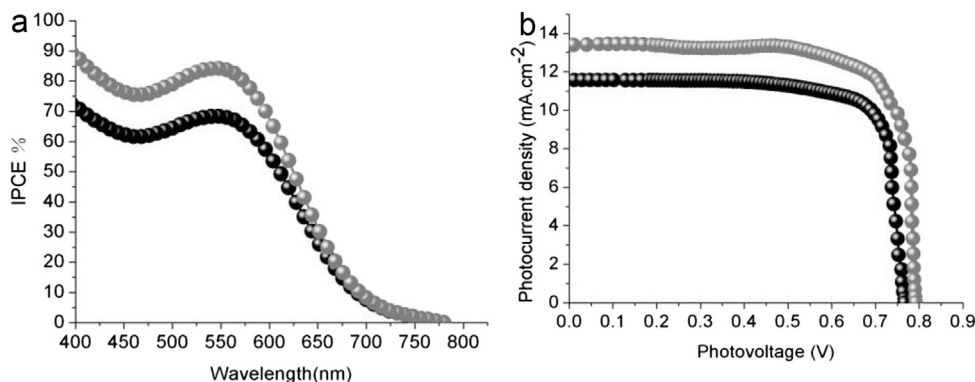


Fig. 3. IPCE (a) and Photocurrent–voltage characteristics (b) of solar cells based on TiO₂ films sensitized with Z907. INCNCs film = gray, TiO₂ nanoparticulate film = black.

films are taken into account, the marked enhancement in the IPCE value for INCNCs electrode result predominantly from the increased charge collection efficiency η_{cc} of the INCNCs TiO₂ electrode. The η_{cc} for the INCNCs electrode is described by the relation $\eta_{cc} = 1 - (\tau_c/\tau_r)$ [24]. The calculated η_{cc} at the highest light intensity ($8.16 \times 10^{16} \text{ cm}^{-2} \text{ s}^{-1}$) in Fig. 2 for the INCNCs electrode film was 13.4% larger than that of the nanoparticulate electrode film, while that at the lowest light intensity ($1.42 \times 10^{15} \text{ cm}^{-2} \text{ s}^{-1}$) for the INCNCs electrode film was 17.3% larger than that of the nanoparticulate electrode film.

Fig. 3b shows the J–V characteristics of the INCNCs electrode with thickness of 6.5 μm . An overall solar conversion efficiency of 8.20% was achieved, with an open circuit voltage (V_{OC}) of 0.793 V, short circuit current density (J_{SC}) of 13.39 mA cm^{-2} , and fill factor (FF) of 0.772. For comparison, the characteristics of a TiO₂ electrode composed of nanoparticles sensitized with Z907 molecules were also measured under similar conditions. The nanoparticulate solar cell exhibited FF = 0.771, J_{SC} = $11.577 \text{ mA cm}^{-2}$, and V_{OC} = 0.767 V, yielding a solar conversion efficiency of 6.84%. The solar conversion efficiency of DSSCs with a INCNCs electrode is about 20% higher than that containing the nanoparticulate electrode. This high light-to-electricity conversion was attributed to the structure of TiO₂ interconnected nanowires consisting of nanosized crystallites shown in Fig. 1, which supplied a large surface area as large as that of a nanoparticulate electrode for the adsorption of Z907 molecules to yield a high IPCE value. The amount of adsorbed dye on the INCNCs film is $4.7 \times 10^{-8} \text{ mol cm}^{-2}$ and on the nanoparticulate film is $4.9 \times 10^{-8} \text{ mol cm}^{-2}$. Because the INCNCs and nanoparticulate photoelectrodes had comparable Z907 dye coverage and were exposed to the same redox electrolyte, it is reasonable to presume the similar initial number of photogenerated carriers for the INCNCs and nanoparticle photoelectrode. Thus, the enhancement of the conversion efficiency must predominantly result from important differences in the charge collection efficiency of the INCNCs film.

4. Conclusion

In summary, densely packed INCNCs were successfully prepared on FTO coated glass substrates via a low temperature hydrolysis reaction. The synthesis method appears general, one that could be readily extended to the synthesis of other metal oxide semiconductors in a nanowire form, given a suitable precursor and interface reaction. For a given film thickness, the INCNCs had shorter electron transport time and several times slower recombination than those of a nanoparticle photoelectrode, indicating

that the charge-collection efficiency of the INCNCs photoelectrodes was extraordinarily enhanced. Dye sensitized solar cells fabricated using the TiO₂ INCNCs film demonstrate very encouraging photo-conversion efficiency, 8.20% of the TiO₂ INCNCs film when using Z907 dye, much higher than 6.84% of TiO₂ nanoparticulate electrode film with same thickness (6.5 μm).

Acknowledgment

This work was supported by the Science and Technology Research Projects of the Education Office of Anhui Province (No. KJ2012Z348).

References

- [1] B.C. O'Regan, S. Scully, A.C. Mayer, J. Phys. Chem. B 109 (2005) 4616–4623.
- [2] W. Juangang, S. Yunli, Appl. Phys. Lett. 102 (2013) 143113–143116.
- [3] F. Fabregat-Santiago, G. Garcia-Belmonte, I. Mora-Sero, J. Bisquer, Phys. Chem. Chem. Phys. 13 (2011) 9083–9118.
- [4] A. Hagfeldt, G. Boschloo, L.C. Sun, L. Klöö, H. Pettersson, Chem. Rev. 110 (2010) 6595–6663.
- [5] B. O'Regan, M. Grätzel, Nature 353 (1991) 737–740.
- [6] S. Hore, E. Palomares, H. Smit, N.J. Bakker, P. Comte, P. Liska, K.R. Thampi, J.M. Kroon, A. Hinsch, J.R. Durrant, J. Mater. Chem. 15 (2005) 412–418.
- [7] W. Juangang, L. Lihua, ECS Electrochem. Lett. 3 (2014) H5–H7.
- [8] B. Lee, D.B. Buchholz, P.J. Guo, D.K. Hwang, R.P.H. Chang, J. Phys. Chem. 11 (2011) 9787–9796.
- [9] F. Xiaojuan, P.D. David, M.S.J. Jessica, T. Akhilesh, R.J.O. Scott, Appl. Phys. Lett. 92 (2008) 193108–193110.
- [10] Z. Dongshe, A. Jonathan Downing, J.K. Fritz, L.M. Jeanne, J. Phys. Chem. B 110 (2006) 21890–21898.
- [11] W. Juangang, C. Tiedan, Mater. Lett. 124 (2014) 302–305.
- [12] M. Zukalova, A. Zukal, L. Kavan, M.K. Nazeeruddin, P. Liska, M. Grätzel, Nano. Lett. 5 (2005) 1789–1792.
- [13] W. Juangang, C. Tiedan, J. Appl. Phys. 115 (2014) 134504(1)–134504(4).
- [14] J.R. Jennings, Y.R. Liu, Q. Wang, J. Phys. Chem. C 115 (2011) 15109–15120.
- [15] G.K. Mor, K. Shankar, P. Maggie, K.V. Oommen, A.G. Craig, Nano Lett. 6 (2006) 215–218.
- [16] R.R. Sonia, F. Fabregat-Santiago, Phys. Chem. Chem. Phys. 15 (2013) 2328–2336.
- [17] Z. Qifeng, P.C. Tammy, R. Bryan, A. Samson Jenekhe, C. Guozhong, Angew. Chem. Int. Ed. 47 (2008) 2402–2406.
- [18] C. Longo, A.F. Nogueiraand, M.A.D. Paoli, J. Phys. Chem. B 106 (2002) 5925–5930.
- [19] E. Stathatos, P. Lianos, A.S. Vukand, B. Orel, Adv. Funct. Mater. 14 (2004) 45–48.
- [20] C. Zhigang, Y. Hong, L. Xianghong, L. Fuyou, Y. Tao, H. Chunhui, J. Mater. Chem. 17 (2007) 1602–1607.
- [21] J.A. Boecker, E. Enache-Pommer, E.S. Aydil, Nanotechnology 19 (2008) 095604–095614.
- [22] R.H. Tao, J.M. Wu, H.X. Xue, X.M. Song, X. Pan, X.Q. Fang, X.D. Fang, S.Y. Dai, J. Power Sources 195 (2010) 2989–2995.
- [23] N.G. Park, G. Schlichthoörl, J. vande Lagemaat, H.M. Cheong, A. Mascarenhas, A.J. Frank, J. Phys. Chem. B 103 (1999) 3308–3314.
- [24] L.J. Vande, A.J. Frank, J. Phys. Chem. B 105 (2001) 11194–11205.